

# CONTINUOUS EDGE GRADIENT-BASED TEMPLATE MATCHING FOR ARTICULATED OBJECTS

Daniel Mohr, Gabriel Zachmann

*Clausthal University, Germany, dmoh@tu-clausthal.de, zach@tu-clausthal.de*

Keywords: template matching, deformable object detection, confidence map, edge feature, graphics hardware

Abstract: In this paper, we propose a novel edge gradient based template matching method for object detection. In contrast to other methods, ours does not perform any binarization or discretization during the online matching. This is facilitated by a new continuous edge gradient similarity measure. Its main components are a novel edge gradient operator, which is applied to query and template images, and the formulation as a convolution, which can be computed very efficiently in Fourier space.

We compared our method to a state-of-the-art chamfer based matching method. The results demonstrate that our method is much more robust against weak edge response and yields much better confidence maps with fewer maxima that are also more significant. In addition, our method lends itself well to efficient implementation on GPUs: at a query image resolution of  $320 \times 256$  and a template resolution of  $80 \times 80$  we can generate about 330 confidence maps per second.

## 1 INTRODUCTION

Detection and tracking of articulated objects is used in many computer vision applications. Our long-term goal is precise tracking of the human hand in order to be able to use it as a dextrous input device for virtual environments and many other applications.

An important initial step in object tracking is to localize the object in the 2D image delivered by the camera. This is a challenging task especially with articulated objects, due to the huge state space and, possibly, time constraints. Most approaches formulate tracking of articulated objects as detecting multiple objects: given a database of many objects, find the object from the database that best matches the object shown in the input image. This also involves finding the location in the input image where that best match occurs. Typically, the database consists of images, called *templates*. This can result in a database size of thousands of templates. A powerful method to match templates is to compare the edge images of template and input image.

In this paper, we propose a novel method for template matching based on edge features, which is robust against varying edge response. To this end, we propose a novel similarity measure between a template and the query image that utilizes the continuous edge gradient (orientation *and* intensity). The input to our algorithm is a query image and a set of templates. The output is a *confidence map*. It stores for each position in

the query image the index and similarity of the best matching template. In subsequent steps, this confidence map can be used directly to extract the best match, or it can be combined with other confidence maps using different features. This is, however, not our focus here.

Our method does *not perform any binarization* or discretization during the online matching process. By contrast, all current methods based on edge distance/similarity need binary edge images. This incurs thresholds that are difficult to adjust automatically, which reduces the robustness of these approaches.

We utilize the *orientation and intensity* of edges of both the templates and the query images directly in our similarity measure. By contrast, most current methods discretize edge orientations into a few intervals, which renders the similarity measure discontinuous with respect to rotation of the object.

Our method is well suited for a complete implementation in the *stream processing model* (e.g., on modern GPUs), which allows for extremely fast template matching.

## 2 RELATED WORK

The most often used edge based approaches to template matching in the field of articulated object detection use the chamfer (Barrow et al., 1977) and Hausdorff (Huttenlocher et al., 1993) distance. Chamfer matching for tracking of articulated objects is, for example, used by (Athitsos

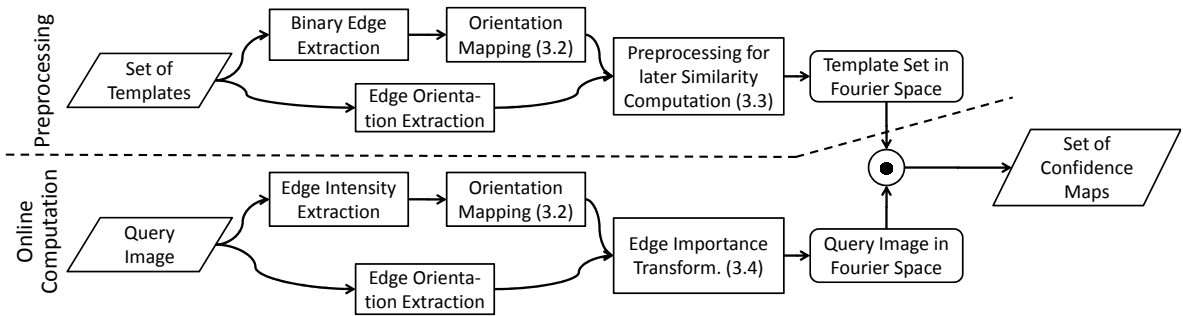


Figure 1: Overview of our approach. The numbers in parentheses denote the section describing the respective stage.

and Sclaroff, 2001) and (Gavrila and Philomin, 1999), the Hausdorff distance by (Olson and Huttenlocher, 1997). The generalized Hausdorff distance is more robust to outliers. The chamfer distance can be implemented as convolution, when used to generate a confidence map. Thus, it can be computed much faster. Both, chamfer and Hausdorff distance can be modified to take edge orientation into account with limited accuracy. One way to do this is to split the template and query images into  $b$  separate images. Each contains only edge pixels within a predefined orientation interval. (Thayananthan et al., 2006), (Stenger et al., 2006). To achieve some robustness against outliers, (Stenger et al., 2006) additionally limited the nearest neighbor distance by a predefined upper bound. A disadvantage of these approaches is, the discretization of the edge orientations, which can cause wrong edge distance estimations.

(Olson and Huttenlocher, 1997) integrated edge orientation into the Hausdorff distance. They modeled each pixel as a 3D-vector, containing pixel coordinates and edge orientation. The maximum norm is used to calculate the pixel-to-pixel distance. (Sudderth et al., 2004) presented a similar approach to incorporate edge position and orientation into chamfer distances. Because it cannot be formulated as convolution, it results in high computation times. Edge orientation information is also used by (Shaknarovich et al., 2003) as a distance measure between templates. They discretized the orientation into four intervals and generate an orientation histogram. They do not take the edge intensity into account. Consequently the weight of edge orientations resulting from noise is equal to that of object edges. This results in a very noise sensitive algorithm.

### 3 The Continuous Edge Image Similarity Measure

Before describing our approach, we introduce the following notation:

$\mathcal{T} = \{T_k \mid k = 0 \dots l - 1\}$  is a set of templates,  $W_k \times H_k$  is the size of  $T_k$ ,  $E_{T_k}$  is the binarized edge image of  $T_k$ ,  $I_Q$  a query image of size  $W_Q \times H_Q$ ,  $I_Q^{\mathbf{O},k} \subset I_Q$  a sub-image of size  $W_k \times H_k$  and centered at  $\mathbf{O} \in [0, W_Q] \times [0, H_Q]$ ,  $E_Q$  the edge intensity image of  $I_Q$ , and  $\mathcal{S}_{I_Q}(k, \mathbf{O})$  a similarity measure between  $I_Q^{\mathbf{O},k}$  and  $T_k$  with the co-domain  $[0, 1]$ , in the sense that the value 1 indicates a perfect match.

The goal of a template matching algorithm is to find the template index  $\bar{k}$  that is most similar to the target object in the image and its correct image coordinates  $\bar{\mathbf{O}}$ . This can be achieved in two steps: First, calculate the image similarities for some or all  $\mathbf{O}$  and  $k$ . Second, based on the similarities, obtained in step 1, choose an appropriate  $\bar{k}$  and  $\bar{\mathbf{O}}$  to represent the object state and position. The latter is not the focus of this paper.

Due to loss of information salient features are needed to get results of high quality. Edges are such a feature. They are fairly robust against illumination changes and varying object color. However, edges are not completely independent from illumination, color, texture, and camera parameters. Therefore, a robust algorithm for efficient template matching is needed.

#### 3.1 Overview of our Approach

Our approach consists of two stages. First, the template set  $\mathcal{T}$  and the query image  $I_Q$  are pre-processed to allow efficient edge-based template matching; second, the matching itself is per-

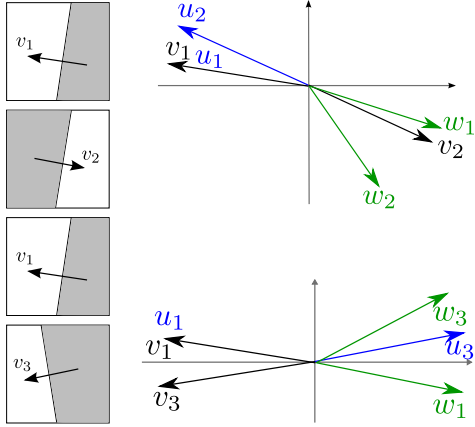


Figure 2: In order to achieve a consistent gradient distance, we map gradients as shown here, before actually comparing them. That way, our edge similarity measure returns low “distances” for the edge gradients in both situations shown here. The  $v_i$  denote the original gradients,  $u_i$  are intermediate ones, and  $w_i$  are the final ones that are further used.

formed, which computes a similarity value for all templates  $T_k$  and all sub-images  $I_Q^{\mathbf{O},k}$  for all query image pixels  $\mathbf{O}$ .

The templates are preprocessed in two steps. First, we generate images of the object in different states and viewpoints. An edge extractor is used to obtain a binary edge image. Then, we extract the edge gradient at the edge pixels. This gradient is then mapped in a way so that they can be compared easily and correctly. Second, we transform the template image such that the similarity between template and query image can be calculated efficiently by a convolution (Section 3.2).

Before computing similarities, we extract the edge intensities and gradients from the query image and map them, just like the preprocessing for the templates. In order to overcome the problem of multiple edges, caused by noise, shadows, and other effects, we further transform the image appropriately.

### 3.2 Computing the Similarity of Edge Images

In this section, we describe the core of our approach, the matching of a template  $T_k$  and a query image  $I_Q$ . We assume we are given the following information:

$L_{T_k} = \{\mathbf{O} \mid E_{T_k}(\mathbf{O}) = 1\}$ , the edge pixel list;  
 $\hat{G}_T$  and  $\hat{G}_Q$ , the mapped edge gradients of the template and query image, resp., additionally each vector normalized to length one;

$\mathcal{N}(\mathbf{x}) = \{\mathbf{x} + \mathbf{y} \mid \mathbf{y} \in [-n, n]^2\}$ ,  $n \in \mathbb{N}$ , a neighborhood of  $\mathbf{x}$ ;

$K$ , a unimodal function (kernel function) with the maximum at  $K(0) = 1$ , and

$K_n$ , a kernel function with bounded support:

$$K_n(\Delta, h) = \begin{cases} K(\frac{\Delta}{h}) & \|\Delta\|_\infty \leq n \\ 0 & \text{otherwise} \end{cases} \quad (1)$$

First we map the image edge gradients such that they can be compared by a simple multiplication without any loss of accuracy. The mapping function  $\hat{\mathbf{v}} = f(\mathbf{v})$  is defined as follows:

$$\theta = \arctan \frac{v_y}{v_x} \quad (2)$$

$$\theta' = \begin{cases} \theta & \theta \geq 0 \\ \theta + \pi & \theta < 0 \end{cases} \quad (3)$$

$$\hat{\mathbf{v}} = (\hat{v}_x, \hat{v}_y) = \|\mathbf{v}\|_2 \cdot (\cos(2\theta'), \sin(2\theta')) \quad (4)$$

Figure 2 illustrates the problem and our mapping.

As explained previously, we do not have a discrete set of edge pixels in the query image, and, thus, cannot calculate directly a distance from each edge pixel  $\mathbf{e} \in L_{T_k}$  to the closest edge pixel in  $I_Q$ . Instead, we use probabilities to estimate the distance: the higher the probability and the nearer a pixel in the query image is to a template edge pixel, the lower the distance should be. The mean probability of a neighborhood of  $\mathbf{e}$  is used as inverse distance measure, so that a small distance results in a high mean value and vice versa. The weight of the neighboring pixels is controlled by the choice of the kernel function  $K$  and its parameter  $h$ . Because only close pixels are relevant for the similarity measure, we only take into account a neighborhood of each template edge pixel of size  $n \in \mathbb{N}$ .

To compute the similarity  $\mathcal{S}_{I_Q}(k, \mathbf{O})$ , we calculate for each edge pixel  $\mathbf{e}$  in the template image the probability  $P^{\mathbf{O},k}(\mathbf{e})$  that an edge in the query image is close to it:

$$P^{\mathbf{O},k}(\mathbf{e}) = \frac{1}{2} + \frac{1}{C_K} \sum_{\mathbf{p} \in \mathcal{N}(\mathbf{e})} \left[ K_n(\mathbf{p} - \mathbf{e}, h) \cdot E_Q(\mathbf{O} + \mathbf{p}) \hat{G}_T(\mathbf{e}) \cdot \hat{G}_Q(\mathbf{O} + \mathbf{p}) \right] \quad (5)$$

with the normalization factor

$$C_K = 2 \cdot \sum_{\mathbf{p} \in \mathcal{N}(\mathbf{e})} K_n(\mathbf{p} - \mathbf{e}, h) \quad (6)$$

Note that  $\hat{G}_T(\mathbf{e}) \cdot \hat{G}_Q(\mathbf{O} + \mathbf{p})$  is a 2D scalar product; because this is in  $[-1, 1]$ , we have to use an

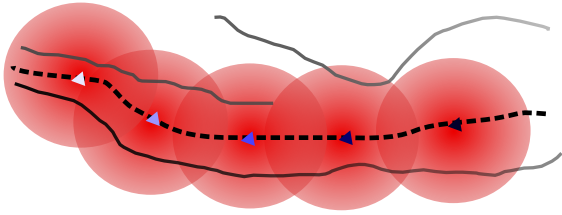


Figure 3: We estimate the similarity between a template edge (dashed line) and a query image edge, which is represented by intensities (gray solid curves), by multiplying a kernel that is centered around each template edge pixel (circles) with the edge intensities. The intensity value of the template edge pixel (triangles) visualize the “closeness” of query image edges.

offset. Figure 3 illustrates the idea behind this measure.

Then, we define the overall similarity as the mean probability

$$\mathcal{S}_{I_Q}(k, \mathbf{O}) = \frac{1}{|L_{T_k}|} \sum_{e \in L_{T_k}} P^{\mathbf{O}, k}(\mathbf{e}) \quad (7)$$

Since the kernel function  $K$  and parameters  $h$  and  $n$  are fixed, the normalization factor  $C_K$  is constant. We insert Eq. 5 into Eq. 7 and rewrite to

$$\mathcal{S}_{I_Q}(k, \mathbf{O}) = \frac{1}{2} + \frac{1}{|L_{T_k}|} \sum_{e \in L_{T_k}} \sum_{\mathbf{p} \in \mathcal{N}(\mathbf{e})} \eta_T(\mathbf{p}, \mathbf{e}) \eta_Q(\mathbf{O} + \mathbf{p}) \quad (8)$$

with

$$\eta_T(\mathbf{p}, \mathbf{e}) = C_K^{-1} K_n(\mathbf{p} - \mathbf{e}, h) \hat{G}_T(\mathbf{e}) \quad (9)$$

$$\eta_Q(x) = E_Q(x) \hat{G}_Q(x) \quad (10)$$

Because  $K_n$  is zero everywhere outside its support, we can rewrite the inner sum as a sum over all pixels in  $T_k$ . Similarly, the outer sum can be rewritten, yielding We rewrite again:

$$\frac{1}{2} + \sum_{\mathbf{x} \in D_k} \left( \eta_Q(\mathbf{O}, \mathbf{x}) \underbrace{\frac{1}{|L_{T_k}|} \sum_{\mathbf{y} \in D_k} E_{T_k}(\mathbf{y}) \eta_T(\mathbf{x}, \mathbf{y})}_{\tilde{E}_{T_k}(\mathbf{x})} \right) \quad (11)$$

where  $D_k = [0, W_k] \times [0, H_k]$ . Notice that  $\tilde{E}_{T_k}$  can be calculated offline. Finally, we arrive at

$$\mathcal{S}_{I_Q}(k, \mathbf{O}) = \frac{1}{2} + \sum_{\mathbf{x} \in D_k} \eta_Q(\mathbf{O} + \mathbf{x}) \cdot \tilde{E}_{T_k}(\mathbf{x}). \quad (12)$$

$\mathcal{S}_{I_Q}(k)$  is called the *confidence map* of  $I_Q$  and  $T_k$  and is basically generated by correlating  $\tilde{E}_{T_k}$  with  $E_Q \hat{G}_Q$ . The image  $\tilde{E}_{T_k}$  is flipped. Then it can be calculated efficiently in Fourier space by

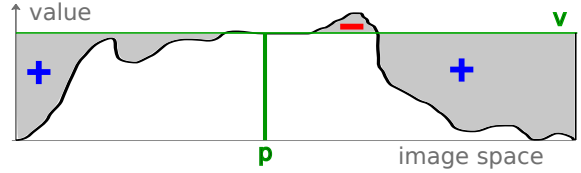


Figure 4: 1D example of our quality measure: the true location  $p$  of the target object is determined manually,  $v_p$  is the value in the combined confidence map. Our quality measure is basically the sum of the signed gray areas over the whole confidence map.

a convolution. Since  $\eta_T, \eta_Q \in \mathcal{R}^2$ , we compute Eq. 12 independently for each component,  $x$  and  $y$ , so that they are scalar-valued correlations.

So far, we have described a robust and fast method to compute the edge similarity between a query image and a set of templates. One remaining problem is that a query image often contains multiple edges close to each other, which are, therefore, also close to the appropriate template edge. For instance, a cable, which produces a shadow, causes four instead of two strong edges. Depending on the edge orientation, this causes severe over- or underestimation of  $P^{\mathbf{O}, k}(\mathbf{e})$ . To overcome this problem, we preprocess the query image. We use the maximum of edge intensity weighed kernels as new intensity. The orientations are calculated as the intensity weighted average of the neighborhood. Due to space limitations we have to refer to our technical report (Mohr and Zachmann, 2009) for a detailed description.

The final template matching process is implemented very efficiently as convolution using the CUDA programming environment (Nvidia, 2008). For more details please take a look at (Mohr and Zachmann, 2009).

## 4 Results

In our datasets, we use the human hand as the object to be detected. In this research field, the chamfer based matching is the most often used. Therefore, we compare our method with the chamfer matching algorithm.

For comparison, we need an appropriate measure for the ability of the methods to localize an object at the correct position in the query image. Given a query image  $I_Q$ , both the chamfer and our method generate a confidence map  $\mathcal{S}_{I_Q}(k)$  for each template  $T_k$ . Now let  $(\hat{x}, \hat{y})$  be the true location of the object in the query image. The matching value at  $(\hat{x}, \hat{y})$  of the template, delivering the

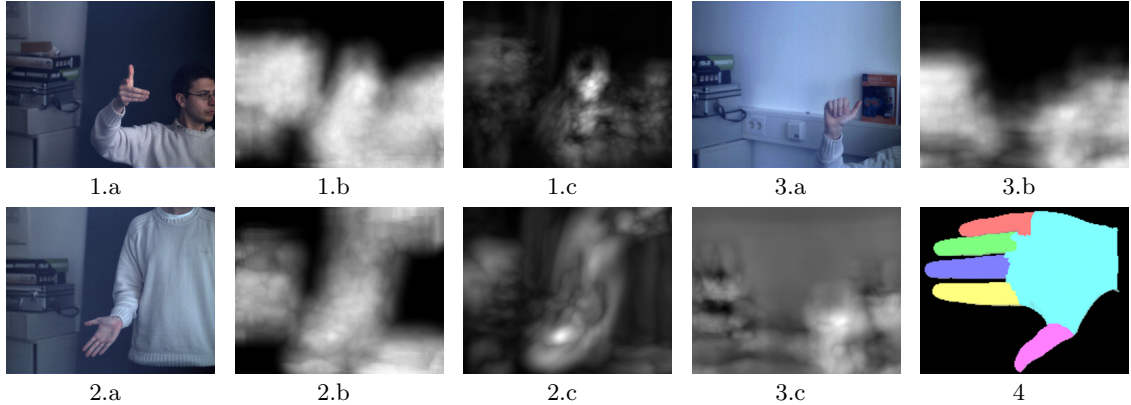


Figure 5: One frame of each of our three datasets: pointing hand (1.), open hand (2.), open-close gesture (3.). The original images are denoted with the letter a, the combined confidence map generated by chamfer matching with b, and those generated by our approach with c. Notice that with our approach, the maxima in our confidence maps are much more significant. Full videos comparing our approach to chamfer matching based confidence maps can be found at <http://cg.in.tu-clausthal.de/research/handtracking/index.shtml> Image 4 shows a rendered template used for matching.

best match according to the approach used, is denoted with  $\hat{c}$ . Obviously, the fewer values in all confidence maps are better than  $\hat{c}$ , the better the matching algorithm is.<sup>1</sup> This is the idea of our quality measure of the matching algorithms. We first define the *combined confidence map*  $\mathcal{S}_{I_Q}$  of  $l$  templates: it stores for each pixel the confidence map value of the template that matches best *at this location*, i.e.

$$\mathcal{S}_{I_Q}(x, y) = \max_{k \in [0, l-1]} \{ \mathcal{S}_{I_Q}(k, x, y) \}. \quad (13)$$

In detail, we use the following quality measure:

$$\mathcal{Q}_{I_Q} = \frac{1}{N} \sum_{\substack{0 \leq x < W_Q \\ 0 \leq y < W_H}} (\mathcal{S}_{I_Q}(\hat{x}, \hat{y}) - \mathcal{S}_{I_Q}(x, y)) \quad (14)$$

with the normalization factor  $N = W_Q H_Q (\max - \min)$ . Min and max are the smallest and largest value in  $\mathcal{S}_{I_Q}$ , resp. We manually determined the true object positions  $(\hat{x}, \hat{y})$ . Thus, the higher the value  $\mathcal{Q}_{I_Q}$ , the better the method works for the query image and template set. Figure 4 illustrates the measure by means of a 1D combined confidence map. The correct template index is not taken into account in the quality measure. But, we observed that at the true position, the best matching template reported by our algorithm looks very similar to the object in the input image in most frames (see URL at Figure 5).

As test data we used RGB images of resolution  $320 \times 256$ . All image preprocessing is done on

<sup>1</sup>The chamfer matching returns distances, not similarities, but the chamfer matching output can be converted easily into similarities by inverting them.

the graphics hardware in CUDA. We used three datasets for evaluation (Figure 5). Dataset 1, consisting of 200 frames, is a pointing hand moving in the image. The templates are 300 renderings of an artificial 3D hand model representing a pointing gesture. Each template is generated from a different camera viewpoint. In dataset 2, an open hand is tested. The length of the dataset is 200 frames, too, and the number of templates is 300 as well. Dataset 3 shows an open-closing sequence of a human hand, consisting of 135 frames. Again, the templates are created using the 3D hand model, with its fingers opening and closing, rendered from three different camera angles. The average template size is about  $80 \times 80$ . As kernel function we have chosen the Gaussian function  $K(x) = e^{-\frac{1}{2}x^2}$ . The bandwidth parameter  $h$ , needed in Eq 1, has been manually optimized; it depends only on the templates, not on the query images. We set  $n = \lceil 3h \rceil$  (three sigma rule for Gaussians) and  $h = 3.3$  for dataset 1 and  $h = 4.0$  for datasets 2 and 3. For the chamfer matching algorithm we used the parameters proposed by (Stenger et al., 2006) (6 edge orientation channels and a distance threshold of 20).

Figure 5 shows an example frame and its combined confidence map for each dataset. Figure 6 shows the quotient  $Q_{GM}/Q_{CF}$  of the quality measure of the two approaches for all frames.  $Q_{GM}$  denotes the quality measure for our approach and  $Q_{CF}$  for the chamfer based approach. Clearly, in most parts of datasets 1 and 3 our approach works better than chamfer based method. Only in the last third of dataset 2, chamfer matching

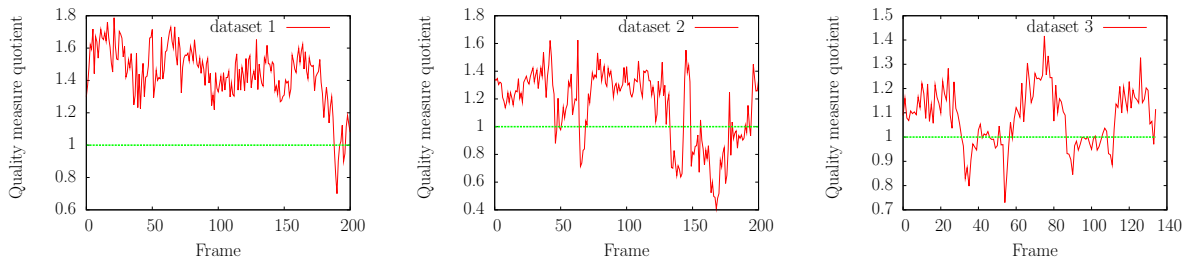


Figure 6: Each plot shows the quotient of the quality between our approach and the chamfer based approach. A value greater than 1 indicates that our approach is better

works better. In these frames, none of the templates matches well the orientation of all fingers. Closer inspection suggests that a lot of orientations in these frames happen to be discretized to the right bin in the chamfer based method. This makes it produce a better match with the right template.

We measured a frame-rate of about 1.1 fps with our datasets. This comprises the preprocessing of the query images and the convolution with 300 templates. The limiting factor of the computation time of the matching process is the FFT. It consumes over 90% of the total time.

## 5 CONCLUSIONS

In this paper, we developed an edge similarity measure for template matching that does not use any thresholds nor discretize edge orientations. Consequently, it works more robustly under various conditions. This is achieved by a continuous edge image similarity measure, which includes a continuous edge orientation distance measure. Our method is implemented as convolution on the GPU and thus is very fast. We generate a confidence map in only 3 ms. The confidence maps can easily be combined with other features to further increase the quality of object detection.

In about 90% of all images of our test datasets, our method generates confidence maps with fewer maxima that are also more significant. This is better than a state-of-the-art chamfer based method, which uses orientation information as well.

In the future, we plan to test anisotropic and asymmetric kernels for the preprocessing of the templates in order to exploit the knowledge of inner and outer object regions. This should improve matching quality. Furthermore, we will research methods to automatically select the kernel bandwidth parameter.

## REFERENCES

- Athitsos, V. and Sclaroff, S. (2001). 3D Hand Pose Estimation by Finding Appearance-Based Matches in a Large Database of Training Views. In *IEEE Workshop on Cues in Communication*.
- Barrow, H. G., Tenenbaum, J. M., Bolles, R. C., and Wolf, H. C. (1977). Parametric Correspondence and Chamfer Matching: Two New Techniques for Image Matching. In *International Joint Conference on Artificial Intelligence*.
- Gavrila, D. M. and Philomin, V. (1999). Real-time Object Detection for Smart Vehicles. In *IEEE International Conference on Computer Vision*.
- Huttenlocher, D., Klanderman, G. A., and Rucklidge, W. J. (1993). Comparing images using the Hausdorff distance. In *IEEE Transactions on Pattern Analysis and Machine Intelligence*.
- Mohr, D. and Zachmann, G. (2009). Continuous Edge Gradient-Based Template Matching for Articulated Objects. In *Technical Report*. <http://cg.in.tu-clausthal.de/publications.shtml>.
- Nvidia (2008). Compute Unified Device Architecture. <http://www.nvidia.com/cuda/>.
- Olson, C. F. and Huttenlocher, D. P. (1997). Automatic Target Recognition by Matching Oriented Edge Pixels. In *IEEE Transactions on Image Processing*.
- Shaknarovich, G., Viola, P., and Darrell, T. (2003). Fast Pose Estimation with Parameter-Sensitive Hashing. In *IEEE International Conference on Computer Vision*.
- Stenger, B., Thayananthan, A., Torr, P. H. S., and Cipolla, R. (2006). Model-Based Hand Tracking Using a Hierarchical Bayesian Filter. In *IEEE Transactions on Pattern Analysis and Machine Intelligence*.
- Sudderth, E. B., Mandel, M. I., Freeman, W. T., and Willsky, A. S. (2004). Visual Hand Tracking Using Nonparametric Belief Propagation. In *IEEE CVPR Workshop on Generative Model Based Vision*.
- Thayananthan, A., Navaratnam, R., Stenger, B., Torr, P., and Cipolla, R. (2006). Multivariate Relevance Vector Machines for Tracking. In *European Conference on Computer Vision*.